Polymer Journal (2025) 57:1067–1081
https://doi.org/10.1038/s41428-025-01064-2

REVIEW

Interface engineering for ternary blend polymer solar cells based on spectroscopic and device analyses

Hideo Ohkita[1]

Received: 30 March 2025 / Revised: 20 May 2025 / Accepted: 21 May 2025 / Published online: 12 June 2025

Abstract

Polymer solar cells, which include a blend of electron-donating conjugated polymers and electron-accepting molecules in the photovoltaic layer, have been widely studied as next-generation solar cells. To improve photocurrent generation, it is necessary to harvest as many photons as possible in solar light, which distributes over a wide wavelength including the ultraviolet, visible, and near-infrared (near-IR) regions. However, covering such a wide solar spectrum by using binary blend polymer solar cells is inherently difficult because most organic materials (e.g., conjugated polymers) have a narrow absorption bandwidth (less than 200 nm). Ternary blend polymer solar cells can overcome this limitation by combining near-IR light-harvesting materials with the electron-donor conjugated polymer and the electron-acceptor molecule. In this review, recent progress in the development of polymer solar cells is briefly overviewed, followed by a detailed description of ternary blend polymer solar cells.

Introduction

Polymer solar cells, which include a photoactive layer consisting of an electron-donating conjugated polymer and an electron-accepting molecule, have significant advantages such as being lightweight, flexible, colorful, and semi-transparent. Therefore, they can be used for a variety of applications that have been difficult to realize with conventional solar cells based on inorganic semiconductors. Furthermore, they can be mass produced via printing technology and thus have the potential to significantly reduce production costs because organic materials are soluble in organic solvents even at room temperature. These advantageous features are also observed in organic semiconductor materials, which are employed not only in organic photovoltaics (OPVs) but also in organic electroluminescence (organic light-emitting diodes (OLEDs)) and organic transistors.

The first OPV, reported by Tang in 1986, was a prototype organic thin-film solar cell based on a bilayer device of a copper phthalocyanine (donor molecule) and a perylene diimide derivative (acceptor molecule) with a conversion efficiency of 1% [1]. One year later, he also reported the first organic electroluminescent device based on a similar bilayer structure [2]. This device converts electrons to photons, in contrast to the OPV device, which converts photons to electrons. In 1991, Hiramoto et al. proposed organic solar cells with a p-i-n structure, which consists of an i-layer based on a mixture of donor/acceptor molecules sandwiched between a p-layer based on donor molecules and an n-layer based on acceptor molecules [3]. In 1995, Heeger et al. reported polymer solar cells based on blends of a conjugated polymer donor and a fullerene acceptor, which were named bulk heterojunction solar cells [4]. In the same year, Friend et al. reported polymer solar cells based on blends of two conjugated polymers as both donor and acceptor materials [5]. This blended layer concept broke through the limitations of bilayer OPVs and has since become the prototype for the basic structure of OPVs. As a result, the power conversion efficiency (PCE) of polymer solar cells has steadily increased, exceeding 20% for tandem cells in 2023 [6] and very recently reaching 21% even for single-junction cells [7] in 2025.

Such efficiency improvements have been realized via research on a variety of aspects, including film formation conditions, synthesis, mechanism understanding, and novel device structures. This research will be described in detail in

✉ Hideo Ohkita
ohkita@photo.polym.kyoto-u.ac.jp

[1] Department of Polymer Chemistry, Graduate School of Engineering, Kyoto University, Katsura, Nishikyo-ku, Kyoto 615-8510, Japan

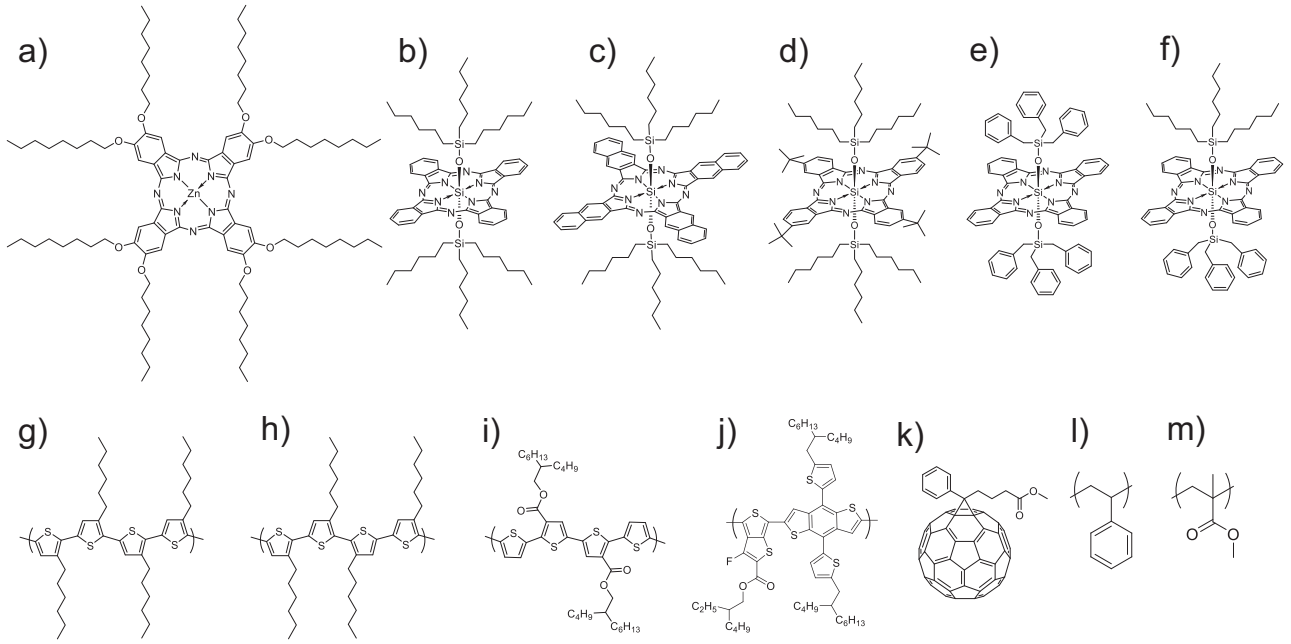

Fig. 1 Chemical structures of all the materials discussed in this review: **a** ZnPc, **b** SiPc6, **c** SiNc6, **d** BuSiPc6, **e** SiPcBz, **f** SiPcBz6, **g** RR-P3HT, **h** RRa-P3HT, **i** PDCBT, **j** PTB7-Th, **k** PCBM, **l** PS, and **m** PMMA

the next section. With respect to the film formation conditions of photoactive layers, blend morphologies suitable for highly efficient photovoltaic performance have been achieved through solvent selection, annealing treatments, and the introduction of additives. With respect to molecular design, a variety of novel materials have been synthesized according to strategies for improving device performance. To improve photocurrent generation, crystalline conjugated polymers with high charge mobility, low-bandgap conjugated polymers with efficient light-harvesting properties in the near-infrared (near-IR) region, acceptor conjugated polymers and nonfullerene acceptor (NFA) molecules with electron-transport and light-harvesting properties have been developed. To improve the open-circuit voltage (V_{OC}), conjugated donor polymers with deeper energy levels of the highest occupied molecular orbital (HOMO) and fullerene derivative acceptors with shallower energy levels of the lowest unoccupied molecular orbital (LUMO) have been developed, thereby increasing the effective bandgap energy in the photoactive layer. On the other hand, the power generation mechanism has also been studied in detail by various measurement techniques, resulting in increased knowledge regarding the molecular assembly structures, electronic structures, and photovoltaic conversion elementary processes. With respect to novel device structures, ternary blend polymer solar cells have been proposed to collect solar light more widely by using near-IR light-harvesting materials with complementary absorption bands, which can overcome limitations in polymer solar cells on the basis of donor/acceptor binary blends. In this review, we

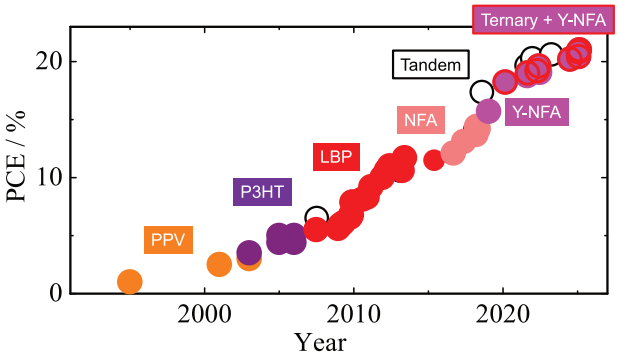

Fig. 2 Recent progress in the PCE of polymer solar cells: PPV-based (orange circles) [4, 5, 8, 9], P3HT-based (purple circles) [10–15], low-bandgap polymer-based (red circles) [16–27], NFA-based (light red circles) [28–32], Y series NFA-based (pink circles) [33–35, 39], Y series NFA-based ternary blends (pink circles with red rings) [7, 36–38, 40, 41], polymer solar cells, and tandem polymer solar cells (black open circles) [6]

briefly describe the progress in the efficiency of polymer solar cells [6–43] and then describe a series of our recent studies on ternary blend polymer solar cells [44–60]. All the materials discussed in this review are summarized in Fig. 1.

Progress in the efficiency of polymer solar cells

As shown in Fig. 2, the PCE of polymer solar cells has increased by more than twenty-fold in the 30 years

since 1995. This is partly because various polymer semiconducting materials have been developed. The PCE has repeatedly increased with each new material developed. The first OPV polymers were poly(*p*-phenylenevinylene) (PPV) derivatives [4, 5, 8, 9], which can collect only a very limited amount of solar light because they were originally studied as OLED materials. Polythiophenes were then employed as the donor material. Interestingly, regioregular poly(3-hexylthiophene) (Fig. 1g: RR-P3HT) can spontaneously form crystalline domains even from solution processing, which are beneficial for efficient light harvesting and charge transport. As a result, the external quantum efficiency (EQE) was increased to more than 80%, and hence, the PCE also increased to more than 4% [10–15]. Polythiophenes can collect solar light over the entire visible region; however, this represents only one-fourth of the total number of photons in the solar light. For further improvements in photocurrent generation, low-bandgap polymers have been developed to harvest solar light in the near-IR region [16–21]. As a result, the PCE has increased to more than 10% [22–27]. However, this approach has a limitation in light harvesting because most organic materials have a narrow absorption bandwidth (up to 200 nm). Therefore, low-bandgap polymers can harvest solar light in the near-IR region but cannot harvest it in the visible region. Unfortunately, a fullerene acceptor (Fig. 1k: PCBM) cannot harvest solar light effectively because of the negligibly low absorption coefficient due to symmetry forbidden transitions. Thus, it is difficult to harvest solar light over a wide wavelength range from the visible to the near-IR region by using polymer solar cells based on binary blends of conjugated polymers and fullerene derivatives. Consequently, as shown in Fig. 2, the increase in the PCE of the polymer solar cells slowed and remained near 10% for a while around 2015. To overcome this limitation, ternary blend polymer solar cells were proposed as a new approach to extend the light-harvesting wavelength range from the visible to the near-IR region [44, 61]. Furthermore, the use of NFA molecules as alternatives to fullerene acceptors has dramatically increased the PCE of polymer solar cells because of their complimentary large absorption in the near-IR region [28–35, 39]. Many recent high-efficiency polymer solar cells with PCE > 19% are based on NFA-based ternary blend photoactive layers [6, 7, 36–38, 40, 41]. As such, the PCE of polymer solar cells has been improved by the continuous development of new photovoltaic materials [42, 43]. Additionally, the ternary blend approach can be considered a second breakthrough in terms of novel device structures after the bulk heterojunction. There have been multiple reviews of ternary blend polymer solar cells [62–73].

Near-IR dye molecules for ternary blend polymer solar cells

Ternary blend polymer solar cells extend the wavelength range of light harvesting by using an additional third near-IR material with an absorption band that is complementary to the original binary blend. Thus, just adding a third-component molecule to the binary blend would improve the efficiency over that of the original binary blend polymer solar cells. However, the process is not so simple. Indeed, no substantial improvement was found for early ternary blend polymer solar cells when using porphyrins and coumarins as a third component [74, 75]. In 2008, Nguyen et al. reported a clear improvement in the efficiency of ternary blend polymer solar cells [61]; at almost the same time, we also reported a ternary blend polymer solar cell with near-IR dye molecules incorporated in RR-P3HT/PCBM blends [44].

Herein, we discuss what structure of near-IR dye molecules can improve the photovoltaic properties of ternary blend polymer solar cells. For comparison, we employed two different near-IR dye molecules – a zinc phthalocyanine (Fig. 1a: ZnPc) and a silicon phthalocyanine (Fig. 1b: SiPc6) – in ternary blend polymer solar cells based on RR-P3HT/PCBM. As shown in Fig. 3, no improvement in the short-circuit current density (J_{SC}) is observed for the RR-

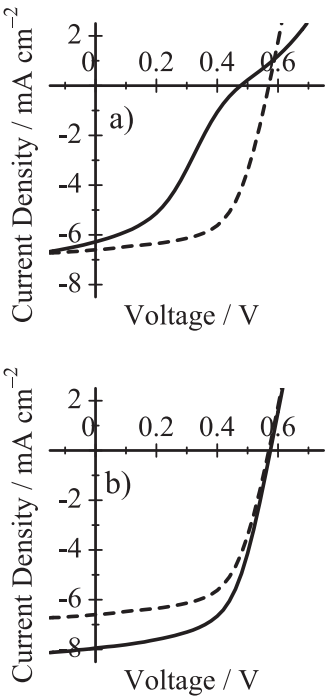

Fig. 3 *J–V* characteristics of ternary and binary blend polymer solar cells: **a** RR-P3HT/PCBM/ZnPc (solid line) and RR-P3HT/PCBM (broken line) and **b** RR-P3HT/PCBM/SiPc6 (solid line) and RR-P3HT/PCBM (broken line). Adapted with permission from Ref. [44]. Copyright 2009 American Chemical Society

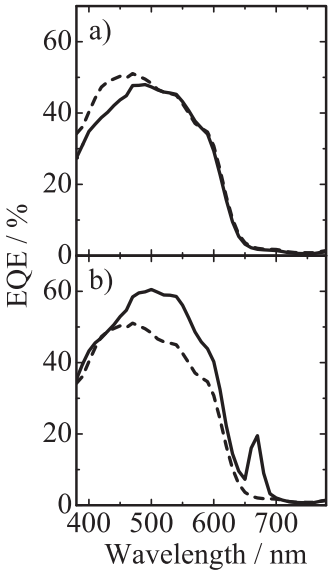

Fig. 4 EQE spectra of ternary and binary blend polymer solar cells: **a** RR-P3HT/PCBM/ZnPc (solid line) and RR-P3HT/PCBM (broken line) and **b** RR-P3HT/PCBM/SiPc6 (solid line) and RR-P3HT/PCBM (broken line). Adapted with permission from Ref. [44]. Copyright 2009 American Chemical Society

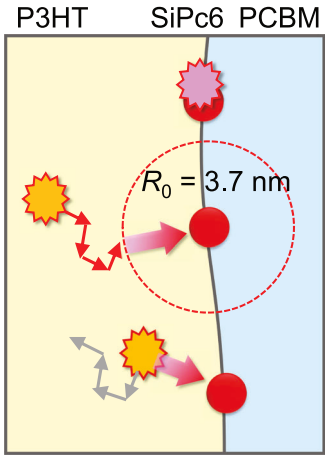

Fig. 5 Schematic illustration of additional light harvesting by near-IR dye molecules at the donor/acceptor interface in ternary blend films: Top) direct absorption of SiPc6 molecules, which can harvest the near-IR light in the solar light that cannot be absorbed by P3HT or PCBM. Middle) Exciton harvesting due to long-range FRET, which can harvest P3HT excitons generated far from the interface more efficiently. Bottom) Exciton harvesting due to long-range FRET from the P3HT energy donor to the SiPc6 energy acceptor, which can more efficiently harvest P3HT excitons that cannot reach the interface by random exciton diffusion

P3HT/PCBM/ZnPc ternary devices, whereas a clear improvement in the J_{SC} is observed for the RR-P3HT/PCBM/SiPc6 ternary devices. For the V_{OC} and fill factor (FF), distinct decreases are observed for the RR-P3HT/PCBM/ZnPc ternary devices, whereas no changes are observed for the RR-P3HT/PCBM/SiPc6 ternary devices. As a result, the PCE is significantly decreased in RR-P3HT/PCBM/ZnPc ternary devices, whereas it is considerably increased in RR-P3HT/PCBM/SiPc6 ternary devices compared with RR-P3HT/PCBM binary devices.

The decrease in the PCE in the RR-P3HT/PCBM/ZnPc ternary devices is due to the lack of improvement in the J_{SC} and the decrease in the FF, leading to a decrease in the $V_{OC.}$ The lack of improvement in the J_{SC} is due to the lack of absorption of ZnPc molecules in the RR-P3HT/PCBM/ZnPc ternary devices; hence, no additional EQE peak is observed in the ZnPc absorption band, as shown in Fig. 4. This finding suggests that ZnPc molecules do not contribute to photocurrent generation. Notably, ZnPc molecules do exist in the ternary blend film because the absorption of ZnPc can be observed again for a solution prepared by redissolving the blend film. This finding indicates excessive aggregation of ZnPc molecules in the ternary blend film, which would disturb charge transport in the blend film and therefore is consistent with the significantly degraded FF mentioned above. In summary, ZnPc molecules with the planar structure are likely to lead to excessive aggregation in the film state and therefore is not suitable for near-IR dye molecules in ternary blend polymer solar cells.

On the other hand, the improved PCE in the RR-P3HT/PCBM/SiPc6 ternary devices is due to the clear improvement in the J_{SC}. As shown in Fig. 4, an additional EQE peak is observed at the SiPc6 absorption band, suggesting that SiPc6 molecules directly contribute to photocurrent generation. Furthermore, the EQE due to the absorption band of RR-P3HT at approximately 400–600 nm also increases with the addition of SiPc6 molecules, indicating that SiPc6 molecules can also indirectly enhance charge generation even upon photoexcitation of RR-P3HT. In other words, as summarized in Fig. 5, there are two mechanisms of photocurrent enhancement based on the direct and indirect contributions of SiPc6 molecules. The direct contribution is the additional absorption of the SiPc6 molecule in the near-IR region, which cannot be absorbed by RR-P3HT or PCBM. The indirect contribution is Förster resonance energy transfer (FRET) from RR-P3HT to SiPc6 at the P3HT/PCBM interface, whereby P3HT excitons are collected at the interface more efficiently than in the binary blend. This FRET method can more efficiently collect P3HT singlet excitons to the interface than exciton diffusion because of the following two effects. One effect is that FRET involves longer-range energy transport than exciton hopping; the other effect is that energy transfer is directed from the P3HT donor to the SiPc6 acceptor, which is different from random hopping by exciton diffusion. As a result, even P3HT singlet excitons generated too far from the interface to reach by exciton diffusion can be efficiently collected at the interface by FRET, resulting in improved photocurrent generation efficiency in the P3HT absorption

band. These sensitization mechanisms will be discussed in more detail later. In summary, SiPc6 molecules with the bulky structure can effectively suppress excessive aggregation in the film state and therefore can contribute to photocurrent generation in ternary blend polymer solar cells. In particular, the hexyl chains of SiPc6 are among the most appropriate bulky ligands for efficient ternary blend polymer solar cells. Shorter or longer alkyl ligands degrade the photovoltaic performance of ternary blend polymer solar cells [45]. The importance of the ligand structure will be discussed in detail in a subsequent section.

Quaternary blend polymer solar cells

Further improvements in J_{SC} can be achieved by using quaternary blend polymer solar cells to expand the light-harvesting wavelength range by using two additional near-IR materials. Therefore, we fabricated quaternary blend polymer solar cells in which two different near-IR dye molecules – namely, SiPc6 and a silicon naphthalocyanine (Fig. 1c: SiNc6) – were simultaneously incorporated into RR-P3HT/PCBM binary blends [46]. Figure 6a shows that the J_{SC} increased by approximately 2 mA cm^{-2} from 9 mA cm^{-2} for the binary device to 11 mA cm^{-2} for the quaternary device, indicating that each near-IR dye molecule increased the J_{SC} by approximately 1 mA cm^{-2}, resulting in a total J_{SC} increase of approximately 2 mA cm^{-2}. As shown in Fig. 6b, two EQE peaks are observed in the SiPc6 and SiNc6 absorption bands, suggesting that both near-IR dye molecules effectively contribute to photocurrent generation. Additionally, as mentioned for the ternary blend device, an improvement in the EQE in the P3HT absorption band is also observed, indicating that the incorporation of near-IR dye molecules contributes to the harvesting of P3HT singlet excitons at the interface by long-range FRET. These results indicate that the light-harvesting wavelength range can be easily extended by simultaneously using multiple near-IR dye molecules with complementary absorption bands. The effective contribution of the incorporation of near-IR dye molecules to photocurrent generation suggests that most near-IR dye molecules are located at the interface between P3HT and PCBM, where excitons can be dissociated into free charge carriers.

Sensitization mechanism in ternary blend polymer solar cells

To understand how many near-IR dye molecules are located at the interface in blend films, we directly observed the sensitization mechanism of the polymer solar cell based on RR-P3HT/PCBM/SiPc6 ternary blends by transient absorption spectroscopy with a short-pulse laser [47]. First, we studied

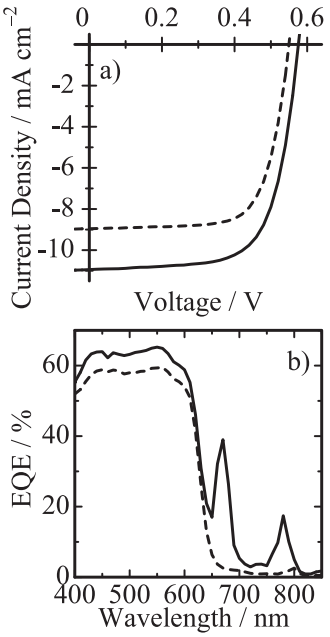

Fig. 6 **a** *J–V* characteristics and **b** EQE spectra of quaternary and binary blend polymer solar cells: RR-P3HT/PCBM/SiPc6/SiNc6 (solid line) and RR-P3HT/PCBM (broken line). Adapted with permission from Ref. [46]. Copyright 2010 Royal Society of Chemistry

how charge generation dynamics are dependent upon the location of near-IR dye molecules in blend films. Upon the photoexcitation of SiPc6 blended in RR-P3HT films, as shown in Fig. 7a, a flat absorption band is observed at 0 ps, which is ascribed to SiPc6 singlet excitons. A large broad absorption band and a small sharp absorption band subsequently increase with a time constant of 2 ps. These large and small absorption bands are attributed to P3HT hole polarons and SiPc6 anions, respectively. In other words, when SiPc6 molecules are located in the P3HT domain, charge generation from SiPc6 singlet excitons has a time constant of 2 ps. On the other hand, upon photoexcitation of SiPc6 blended in PCBM films, as shown in Fig. 7b, no flat absorption band ascribed to SiPc6 singlet excitons is observed; instead, a sharp absorption band is observed at 1010 nm even at 0 ps, which is ascribed to the PCBM anion. This finding shows that when SiPc6 molecules are located in the PCBM domain, charge carriers are promptly generated from SiPc6 singlet excitons within a laser pulse width of 0.2 ps. Note that all the charge carriers generated in either blend finally recombine geminately within a few nanoseconds. In summary, the charge generation dynamics are dependent upon the location of the near-IR dye molecules. Therefore, we can discuss the location of near-IR dye molecules on the basis of the charge generation dynamics measured by transient absorption spectroscopy.

Figure 7c shows the time evolution of the transient absorption spectra of the RR-P3HT/PCBM/SiPc6 ternary blend film upon selective photoexcitation of SiPc6 molecules. Immediately after laser excitation, a flat absorption

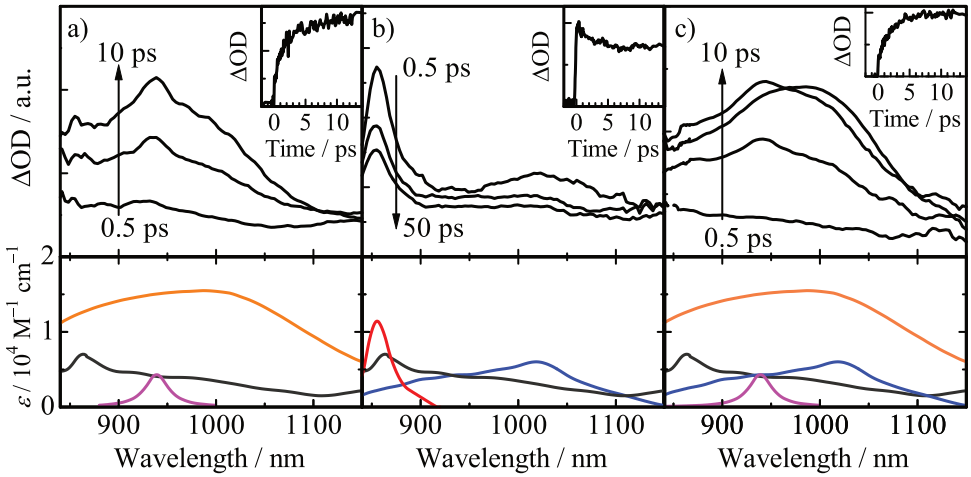

Fig. 7 Top) Transient absorption spectra of binary and ternary blend films upon photoexcitation of SiPc6: **a** RR-P3HT/SiPc6, **b** PCBM/SiPc6, and **c** RR-P3HT/PCBM/SiPc6. Bottom) Absorption spectra of SiPc6 singlet excitons (black lines), P3HT hole polarons (orange lines), SiPc6 anions (purple lines), PCBM anions (blue lines), and SiPc6 cations (red lines). Adapted with permission from Ref. [47]. Copyright 2011 American Chemical Society

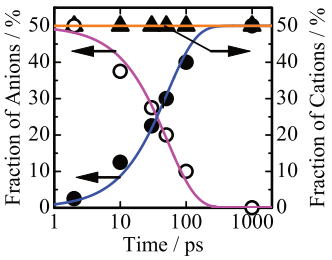

Fig. 8 Time evolution of each transient species in the ternary blend films: SiPc6 anion (open circles with purple lines), PCBM anion (closed circles with blue lines), and P3HT hole polaron (closed triangles with orange lines). Adapted with permission from Ref. [47]. Copyright 2011 American Chemical Society

band is observed first; then, a large broad absorption band and a small sharp absorption band increase with a time constant of 2 ps. This spectral change is the same as that observed for the RR-P3HT/SiPc6 binary blend mentioned above, indicating that SiPc6 molecules are located in the P3HT domain in the ternary blend film. If SiPc6 molecules are isolated in the P3HT domain, as is the case with the RR-P3HT/SiPc binary blend film, P3HT hole polarons and SiPc6 anions would recombine geminately in a few nanoseconds. However, this is not the case. As shown in Fig. 7c, the small absorption band of SiPc6 anions rapidly disappears after tens of picoseconds, and instead, the absorption band shifts to approximately 1000 nm, which is ascribed to the formation of PCBM anions. By analyzing the time evolution of each transient species resolved, as shown in Fig. 8, we find that the time constant is 50 ps for both the decay of the SiPc6 anion and the formation of the PCBM anion. This finding indicates an electron transfer from the SiPc6 anion to the PCBM with a time constant of 50 ps. In summary, charge transfer between P3HT and SiPc6 results in a P3HT hole polaron and SiPc6 anion with a time constant of 2 ps, followed by electron transfer from the SiPc6 anion to PCBM with a time constant of 50 ps. These findings show that SiPc6 molecules are in close contact not only with P3HT but also with PCBM, i.e., at the interface of P3HT and PCBM. Furthermore, the decay of the P3HT hole polaron during this period is negligible in the ternary blend films, indicating that no SiPc6 molecules are isolated in the P3HT domain. We therefore conclude that almost all SiPc6 molecules are spontaneously segregated at the interface between P3HT and PCBM.

Notably, these results are found for thermally annealed blend films, whereas no electron transfer from SiPc6 anions to PCBM is observed in solvent-annealed blend films, and the direct formation of P3HT polarons and PCBM anions from the SiPc6 singlet excitons is observed with a time constant of 2 ps. In other words, the SiPc6 singlet exciton is directly converted to the P3HT polaron and PCBM anion at a time constant of 2 ps. This result suggests that the electron transfer from the SiPc6 anion to the PCBM proceeds faster than the hole transfer from the SiPc6 singlet exciton to the P3HT, which is consistent with the higher sensitization efficiency of the ternary blend device with solvent annealing.

Furthermore, the charge generation dynamics upon photoexcitation of P3HT in the RR-P3HT/PCBM/SiPc6 ternary blend film are notable. In this case, the P3HT singlet exciton decays with a shorter time constant of 4 ps, in addition to a longer time constant of 25 ps, which is also observed for the RR-P3HT/PCBM binary blend film. The shorter decay constant (4 ps) is consistent with the time constant for the increase in breaching in the SiPc6 absorption band. Therefore, this faster decay can be attributed to the FRET from the P3HT singlet exciton to the SiPc6 molecules in the ternary blend film. After our report, similar FRET has been reported in other ternary blend polymer solar cells [52, 72, 76, 77], indicating that exciton harvesting is a versatile advantage in ternary blend polymer

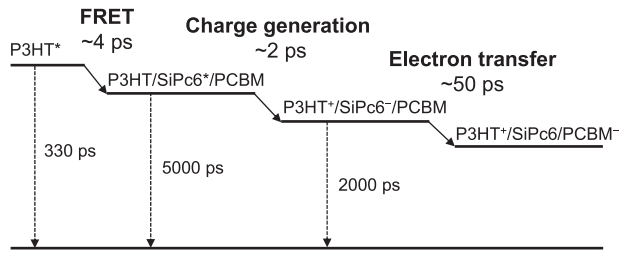

Fig. 9 Energy diagrams of exciton harvesting, charge generation, and electron transfer in RR-P3HT/PCBM/SiPc6 ternary blend films

solar cells in addition to direct absorption. As summarized in Fig. 9, all the charge generation dynamics are considerably faster than the corresponding backward reactions are, which is consistent with efficient charge generation in ternary blend polymer solar cells.

Spontaneous segregation of near-IR dye molecules

As described above, almost all the near-IR dye molecules spontaneously segregate into the P3HT/PCBM interface in the ternary blend films even though the films are only prepared from a blend of the three materials. This result indicates that some driving forces cause dye segregation at the interface. To address the origin of this interfacial segregation, we first evaluated the local concentration of the dye molecules in the blended films by using SiPc6 molecules dispersed in polystyrene (Fig. 1l: PS) films at various concentrations. We found that the absorption peak of SiPc6 shifted in a SiPc6 concentration-dependent manner. In other words, the local concentration of SiPc6 molecules can be evaluated from the absorption peak. Hence, we found that the higher the crystallinity of P3HT is, the higher the local concentration of SiPc6 molecules in P3HT/PCBM/SiPc6 ternary blend films. This result suggests that as P3HT crystalline or PCBM aggregated domains grow, the foreign material SiPc6 is excluded from the crystalline or aggregated domains to the disordered interface. This exclusion effect is analogous to the phenomenon in which slow cooling of seawater results in the formation of freshwater ice from which salt is removed. Interestingly, even when amorphous regiorandom P3HT (Fig. 1h: RRa-P3HT) with zero crystallinity is used, the local concentration of SiPc6 molecules is more than four times higher in RRa-P3HT/PCBM/SiPc6 ternary blends than the concentration expected from a homogeneous distribution, indicating that there are driving forces other than the exclusion effect associated with P3HT crystallization that promote the interfacial segregation of near-IR dye molecules [48].

Therefore, we next focused on the difference in surface energy as the driving force that promotes the interfacial segregation of the near-IR dye molecules in blend films. In a similar study, the location of a third component, such as carbon black, in binary polymer blend films was discussed in terms of surface energy [78]. Let the surface energy of the material X be γ_X, the surface energy of the material Y be γ_Y, and the surface energy of the third component Z be γ_Z. The interfacial energy γ_{XY} for the interface formed by material X and material Y can be calculated by Neumann's equation, $\gamma_{XY} = \gamma_X + \gamma_Y - 2(\gamma_X\gamma_Y)^{0.5} \exp[-\beta(\gamma_X - \gamma_Y)^2]$, where $\beta = 0.000115$ m^4 mJ^{-2} [79]. The wettability of the third component Z to the blend matrix consisting of X and Y materials is called the wetting coefficient $\omega_{Z/XY}$, which is given by $\omega_{Z/XY} = (\gamma_{ZY} - \gamma_{ZX})/\gamma_{XY}$. When the wetting coefficient satisfies $\omega_{Z/XY} < -1$, the Z component is expected to be located in the Y domain. When $-1 < \omega_{Z/XY} < 1$, the Z component is expected to be located at the XY interface. When $\omega_{Z/XY} > 1$, the Z component is expected to be located in the X domain. The wetting coefficient of SiPc6 molecules for RR-P3HT/PCBM blend films is $-1 < \omega_{SiPc6/RR\text{-}P3HTPCBM} = 0.32 < 1$; thus, the SiPc6 molecule is expected to segregate at the interface in terms of the wetting coefficient.

To verify the relationship between the location of near-IR dye molecules in the polymer blend films and the wetting coefficient, RR-P3HT/PS blend films were employed as a model system instead of RR-P3HT/PCBM. This is because polymer blend films are likely to form large phase-separated structures on micrometer scales, which allows us to observe the location of the near-IR dye molecules directly by using atomic force microscopy (AFM). Similar to PCBM, PS has a high surface energy because of the presence of phenyl groups in the side chain and is therefore a suitable model system alternative to RR-P3HT/PCBM blends. The wetting coefficient of the SiPc6 molecules in the RR-P3HT/PS blend film is $-1 < \omega_{SiPc6/RR\text{-}P3HTPS} = 0.60 < 1$, suggesting that SiPc6 molecules are expected to segregate to the P3HT/PS interface in RR-P3HT/PS/SiPc6 ternary blend films, as in RR-P3HT/PCBM/SiPc6 ternary blend films. In the AFM image after spin-coating, sea–island phase-separated structures are observed, as shown in Fig. 10d, and ring-shaped structures are observed at the sea–island interface. The image suggests that this ring-shaped region is brighter and higher than the other regions. After this ternary blend film is immersed in pentane solvent, which can selectively extract only SiPc6 molecules, similar sea–island phase-separated structures are observed, as shown in Fig. 10e. Interestingly, the ring regions, which were high before the pentane treatment, were darker than the other regions were, suggesting that they were lower than the other regions were. A comparison of the absorption spectra before and after the pentane treatment, as shown in Fig. 10a, b, revealed that the SiPc6 absorption bands were at approximately 350, 620 and 680 nm before the treatment but disappeared after the treatment. On the other hand, no change in the P3HT absorption band was

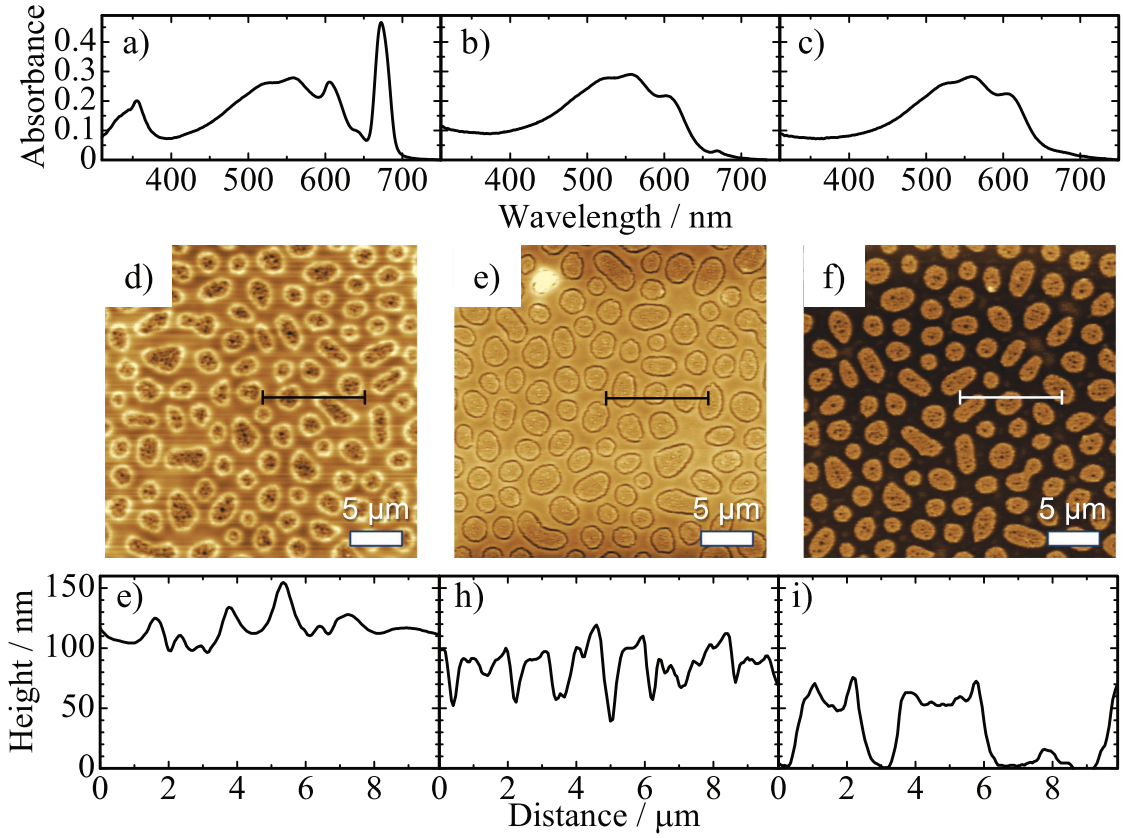

Fig. 10 Top) Absorption spectra, Middle) AFM images, Bottom) Line profiles at the bars in the above AFM images of RR-P3HT/PS/SiPc6 (4:4:2 w/w) ternary blend films: **a, d, g** as cast, **b, e, h** after the pentane treatment, and **c, f, i** after the cyclohexane treatment. The scale bars are shown in the bottom right section of each AFM image. Adapted with permission from Ref. [48]. Copyright 2011 Wiley-YCH Verlag GmbH & Co. KGaA

observed, indicating that only SiPc6 molecules were selectively extracted. These results indicate that the SiPc6 molecules segregate to the ring-shaped part of the interface between P3HT and PS, which is consistent with the location predicted by the wetting coefficient.

We have also studied another ternary blend film of poly(methyl methacrylate) (Fig. 1m: PMMA) and PS with SiPc6, where the order of surface energy is $\gamma_{SiPc6} < \gamma_{PS} < \gamma_{PMMA}$; hence, the wetting coefficient of the SiPc6 molecule in the PMMA/PS blend film is $\omega_{SiPc6/PMMAPS} = -1.3 < -1$, suggesting that SiPc6 molecules are expected to be located in the PS domain in the PMMA/PS/SiPc6 ternary blend films. In the AFM image after spin-coating, sea–island phase-separated structures are observed, as shown in Fig. 11d, but no ring-shaped structures are observed at the sea–island interface. After this ternary blend film was immersed in pentane solvent, as shown in Fig. 11e, the same sea–island phase-separated structures were observed again, but the sea domains became darker, suggesting that they were lower in height than the other regions. A comparison of the absorption spectra before and after the pentane treatment is shown in Figs. 11a and 12b and revealed that the SiPc6 absorption bands at approximately 350, 620, and 680 nm were all reduced after the treatment. This finding indicates that only SiPc6 molecules were selectively extracted from the sea domains. After this ternary blend film was immersed in hexane, which can selectively extract only PS, as shown in Fig. 11f, the sea domains completely disappeared after the treatment, suggesting that the sea domains are ascribable to PS. These results indicate that the SiPc6 molecules are located in the PS domains, which is again consistent with the location predicted by the wetting coefficient. In summary, we can conclude that the interfacial segregation of the near-IR dye molecules in the blend films is due to the interfacial segregation effect caused by the balance of the surface energies of the component materials, in addition to the exclusion effect of the near-IR dye molecules from the interface due to the crystallization or aggregation of the matrix materials.

Considering the studies described above, the location of the near-IR dye molecules in the blend film can be controlled by tuning the surface energy of each material. To demonstrate this, we employed three near-IR dye molecules with different axial ligands (Fig. 1b: SiPc6, Fig. 1d: BuSiPc6, and Fig. 1e: SiPcBz), which have different surface energies, as shown in Fig. 12 [49]. To eliminate the

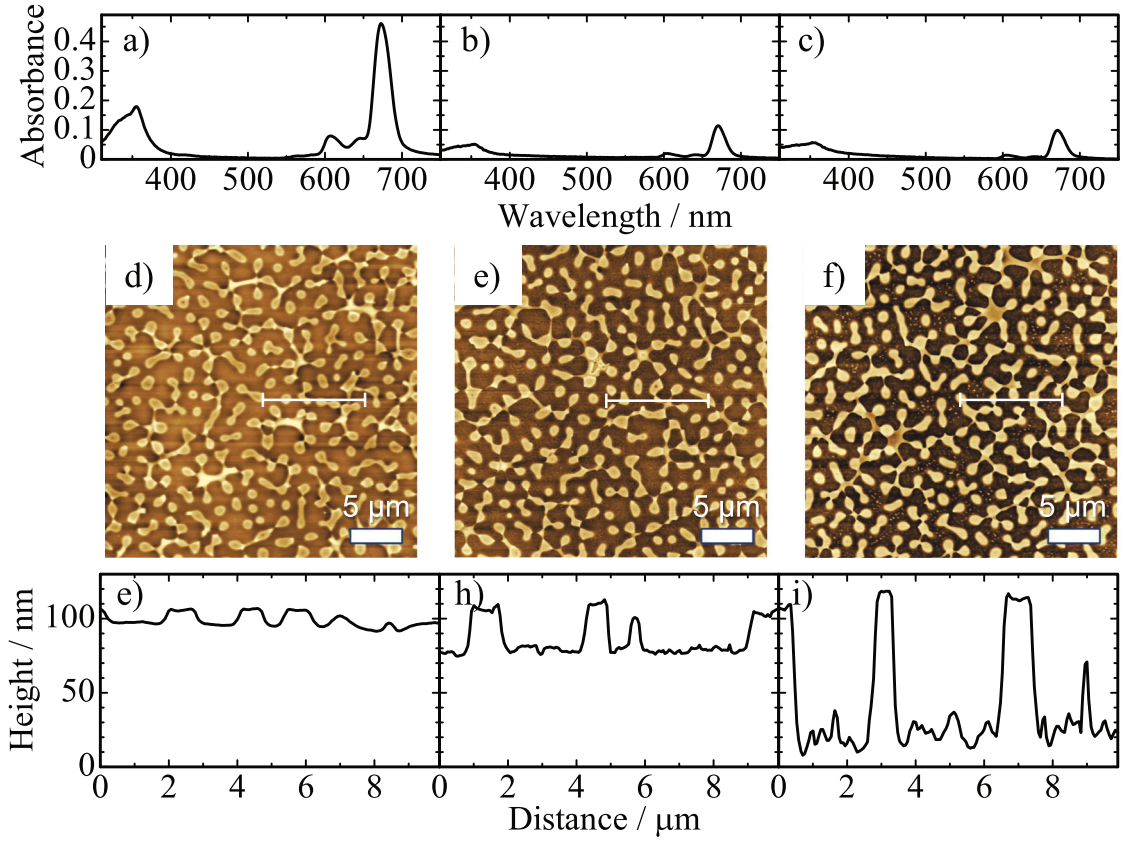

Fig. 11 Top) Absorption spectra, Middle) AFM images, Bottom) Line profiles at the bars in the above AFM images of the PMMA/PS/SiPc6 (4:4:2 w/w) ternary blend films: **a, d, g** as cast, **b, e, h** after the pentane treatment, and **c, f, i** after the cyclohexane treatment. The scale bars are shown in the bottom right section of each AFM image. Adapted with permission from Ref. [48]. Copyright 2011 Wiley-YCH Verlag GmbH & Co. KGaA

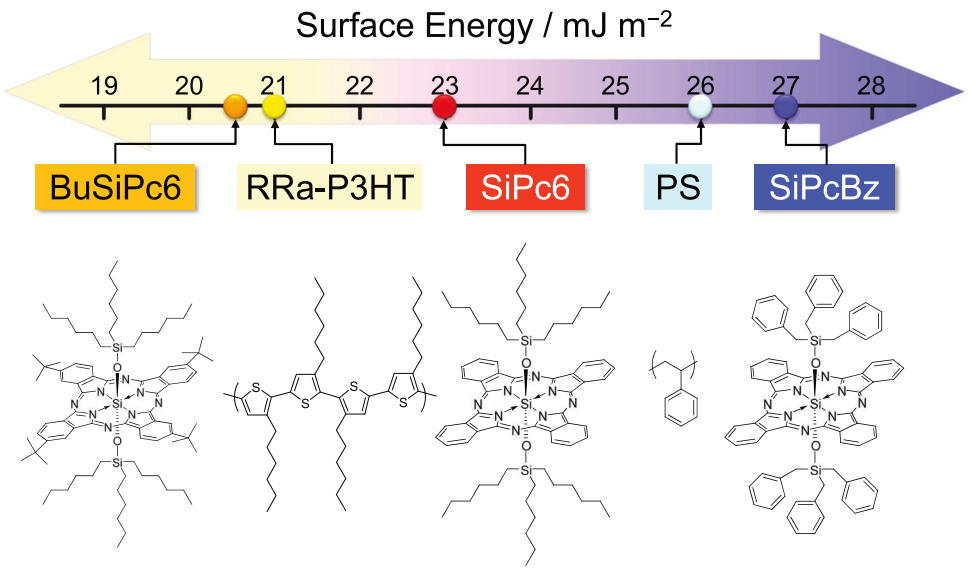

Fig. 12 Surface energy and chemical structures of BuSiPc6, RRa-P3HT, SiPc6, PS, and SiPcBz

exclusion effect of the near-IR dye molecules due to crystallization, RRa-P3HT and PS are employed as matrix polymers. The first one is BuSiPc6, which has hexyl groups to the axial ligand and tertiary butyl groups to the phthalocyanine ring plane. This near-IR dye molecule has the lowest surface energy. The second one is SiPc6, which has hexyl groups to the axial ligand. This has an intermediate surface energy between those of RRa-P3HT and

PS. The third one is SiPcBz, which has benzyl groups to the axial ligand. This has the highest surface energy. Thus, the wetting coefficient for the RRa-P3HT/PS blend film is found to be $\omega_{\mathrm{BuSiPc6/RRa\text{-}P3HTPS}} = 1.2 > 1$ for BuSiPc6, $-1 < \omega_{\mathrm{SiPc6/RRa\text{-}P3HTPS}} = 0.2 < 1$ for SiPc6, and $\omega_{\mathrm{SiPcBz/RRa\text{-}P3HTPS}} = -1.4 < -1$ for SiPcBz. In other words, BuSiPc6 is expected to be located in the RRa-P3HT domains, SiPc6 is expected to be segregated at the RRa-P3HT/PS interface, and SiPcBz is expected to be located in the PS domains. To identify the location of each near-IR dye molecule, we obtained AFM images of each blend film before and after selective extraction of the near-IR dye molecules by pentane treatment. As summarized in Table 1, approximately 90% of all near-IR dye molecules are located at positions predicted by the wetting coefficient. These findings demonstrate that near-IR dye molecules with finely tuned surface energies can be selectively introduced into the intended domains or interfaces of blended films by appropriate molecular design.

Interface engineering for ternary blend polymer solar cells

As described above, ternary blend polymer solar cells are a promising approach that can easily expand the light-harvesting wavelength range and effectively improve the photovoltaic conversion efficiency. However, only a small amount of near-IR dye molecules can be introduced into ternary blend polymer solar cells. The optimal amount introduced is as low as 5 wt%, and further additions degrade device performance. This is probably because the near-IR dye molecules are nonselectively located outside the donor/acceptor interface when they are introduced at high concentrations in ternary blends. Therefore, to maximize the potential of ternary blend polymer solar cells, it is necessary to develop near-IR dye molecules with higher interfacial selectivity than before.

Table 1 Near-IR dye location fraction in RRa-P3HT/PS blend films

Near-IR dye	RRa-P3HT	Interface	PS	Predicted Location
BuSiPc6	87%	13%	—	RRa-P3HT
SiPc6	10%	90%	—	Interface
SiPcBz	—	7%	93%	PS

In the case of silicon phthalocyanine molecules, as described previously, interfacial segregation can be induced by molecular design with appropriate surface energy tuned by designing axial ligands. Considering the modeling studies described in the previous section, the introduction of a hexyl group as an axial ligand can lower the surface energy and make it compatible with P3HT, whereas the introduction of a benzyl group can increase the surface energy and make it compatible with PCBM. Inspired by the high interfacial selectivity of surfactants with both hydrophilic and hydrophobic groups, we synthesized a near-IR dye molecule (Fig. 1f: SiPcBz6) with both hexyl and benzyl ligands that is compatible with both P3HT and PCBM, respectively [50]. Figure 13a shows the photovoltaic properties of the P3HT/PCBM/SiPcBz6 ternary blend polymer solar cells. For devices using the heterostructured near-IR dye SiPcBz6, the photovoltaic performance is maximized when the dye concentration is as high as 15 wt%, which is three times greater than the concentration of homostructured near-IR dye molecules such as SiPc6 and SiPcBz. As a result, J_{SC} increased by 30% from 10 to 13 mA cm^{-2}, and the PCE increased by approximately 30%, from 3.8 to 4.8%. As shown in Fig. 13b, the EQE is as high as 70% in the SiPcBz6 absorption band, which is comparable to that in the P3HT absorption band and is almost double that of conventional homostructured near-IR dye molecules. These results indicate that heterostructured SiPcBz6 dye molecules can self-assemble to spontaneously segregate at the interface at high concentrations. We therefore conclude that the potential of ternary blend devices can be maximized by

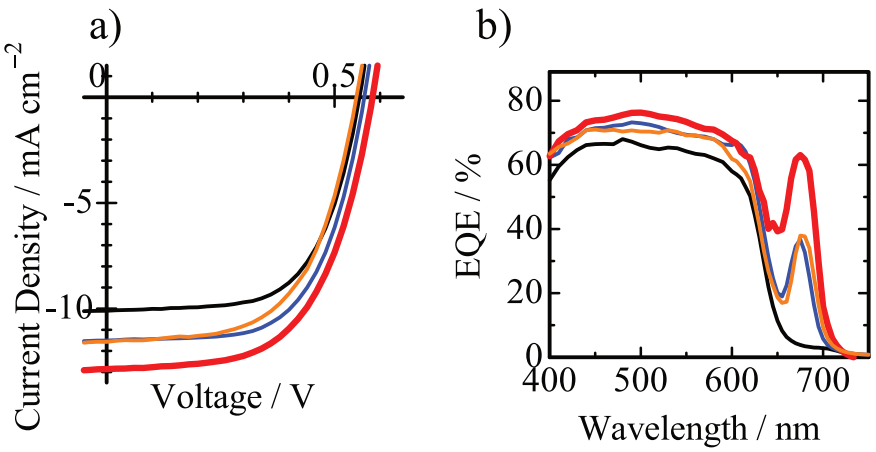

Fig. 13 **a** *J–V* characteristics and **b** EQE spectra of ternary and binary blend polymer solar cells: RR-P3HT/PCBM (black line), RR-P3HT/PCBM/SiPc6 (orange line), RR-P3HT/PCBM/SiPcBz (blue line), and RR-P3HT/PCBM/SiPcBz6 (thick red line). Adapted with permission from Ref. [50]. Copyright 2015 Wiley-YCH Verlag GmbH & Co. KGaA

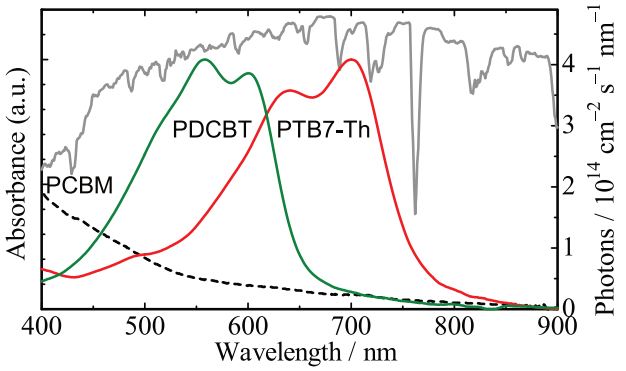

Fig. 14 Absorption spectra of PDCBT (green line), PTB7-Th (red line), and the PCBM broken line). Photon flux spectrum of solar light (gray line). Adapted with permission from Ref. [54]. Copyright 2019 Wiley-YCH Verlag GmbH & Co. KGaA

using near-IR dye molecules with greatly improved interfacial selectivity in ternary blend polymer solar cells by optimizing the molecular structure design.

Improved charge transport

Low-bandgap conjugated polymers can be employed as near-IR materials in ternary blend polymer solar cells. We have studied ternary blend polymer solar cells based on a wide-bandgap conjugated donor polymer (PDCBT), a low-bandgap conjugated donor polymer (PTB7-Th), and a fullerene acceptor (PCBM), as shown in Fig. 14 [53]. Compared with binary blend polymer solar cells based on PTB7-Th and PCBM, as shown in Fig. 15, PDCBT/PTB7-Th/PCBM ternary blend cells exhibit higher J_{SC} and FF values for all thicknesses of the photoactive layer. The higher J_{SC} is due to the complimentary absorption bands of PDCBT and PTB7-Th, which can expand the light-harvesting wavelength range effectively. On the other hand, the higher FF indicates that charge transport is improved in the ternary blend films. Similar improvements in FF have also been reported for some ternary blend polymer solar cells [80–85].

To address the origin of the improved FF, we assign charge carriers in these blend films by transient absorption measurements [54]. Figure 16 shows the transient absorption spectra of the ternary and binary blend films at 5 μs after laser excitation. Since singlet and triplet excitons disappear at this time domain, these long-lived transient species can be attributed to the hole polarons of the donor polymer. Notably, the absorption of the PCBM anion is negligible because of the considerably lower absorption coefficient than that of the hole polarons. The blue line is the transient absorption spectrum of the PDCBT/PCBM binary blend film, which can be ascribed to the PDCBT hole polaron. The red line represents the transient absorption

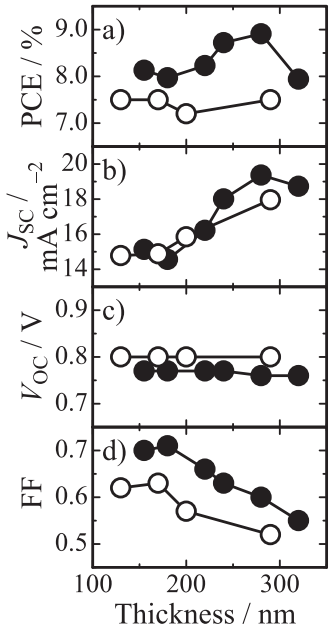

Fig. 15 Photovoltaic parameters of PTB7-Th/PCBM binary (open circles) and PDCBT/PTB7-Th/PCBM ternary (closed circles) blend polymer solar cells plotted against the thickness of the photoactive layer. Adapted with permission from Ref. [53]. Copyright 2018 The Chemical Society of Japan

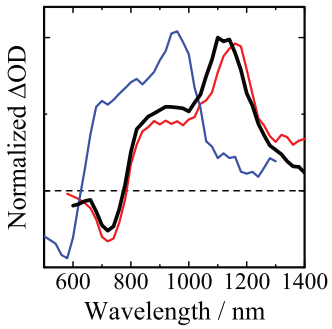

Fig. 16 Transient absorption spectra of PDCBT/PCBM binary (blue line), PTB7-Th/PCBM binary (red line), and PDCBT/PTB7-Th/PCBM ternary blend (black thick line) films excited at 532 nm. Adapted with permission from Ref. [54]. Copyright 2019 Wiley-YCH Verlag GmbH & Co. KGaA

spectrum of the PTB7-Th/PCBM binary blend film, which can be attributed to the PTB7-Th hole polaron. This thick black line is the transient absorption spectrum of PDCBT/PTB7-Th/PCBM ternary blends, which is almost identical to the red line. This agreement indicates that the charge carriers in the ternary blend film are PTB7-Th hole polarons even though PDCBT is selectively excited. This finding clearly shows that the charge carriers are the same in both binary and ternary blends and should be PTB7-Th hole polarons. Nonetheless, hole transport is improved in the ternary blend films. As summarized in Table 2, the hole mobility is the highest in the ternary blend films, even though the volume fraction of PTB7-Th is as small as 30%,

Table 2 Hole mobility of neat, binary and ternary blend films

Samples	Hole mobility / $cm^2\ V^{-1}\ s^{-1}$
PTB7-Th	2.8×10^{-4}
PDCBT	1.3×10^{-4}
PTB7-Th/PCBM	2.4×10^{-4}
PDCBT/PCBM	2.7×10^{-4}
PDCBT/PTB7-Th/PCBM (0.3 : 0.1 : 0.6 w/w)	6.3×10^{-4}

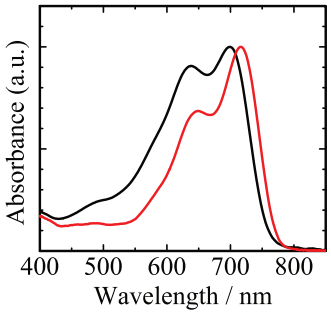

Fig. 17 Absorption spectra of PTB7-Th in the neat film (black line) and in the PDCBT/PTB7-Th/PCBM ternary blend film (red line). The PTB7-Th spectrum of the ternary blend film was obtained by subtracting the PDCBT and PCBM absorption spectra from the original spectrum. The absorption was normalized at the peak. Adapted with permission from Ref. [54]. Copyright 2019 Wiley-YCH Verlag GmbH & Co. KGaA

suggesting that the hole transport in PTB7-Th is greatly improved in the ternary blend films. As shown in Fig. 17, the 0–0 absorption band of PTB7-Th is more clearly observed in the ternary blend than in the neat film. This finding suggests that the PTB7-Th chains are more ordered in the ternary blend than in the neat film. Thus, we consider that ternary blends of the appropriate material combination not only expand the light-harvesting wavelength range but also enhance the hole transport properties by promoting the ordering of the conjugated polymer chains.

Summary and future perspective

In this review, we describe ternary blend polymer solar cells with near-IR dye molecules as a new approach to extend the wavelength range of light harvesting in polymer solar cells. To achieve highly efficient near-IR dye sensitization, near-IR dye molecules must undergo spontaneous segregation at the donor/acceptor interface without reducing the absorbance due to excessive aggregation. Silicon phthalocyanine derivatives with appropriately bulky axial ligands such as SiPc6 are near-IR dye molecules that satisfy these requirements. Therefore, by using these materials as third materials in ternary blend polymer solar cells, the light-harvesting wavelength range can be extended by adding new absorption bands, and the excitons generated in the polymer domain can be efficiently harvested at the interface via long-range FRET. Furthermore, the light-harvesting wavelength range can be easily expanded by multicolored polymer solar cells, in which several near-IR dye molecules with complementary absorption bands are introduced simultaneously. Transient absorption studies have shown that the SiPc6 excitons generated by photoexcitation are converted to SiPc6 anions and P3HT hole polarons with a time constant of 2 ps, followed by the generation of PCBM anions by electron transfer from the SiPc6 anion to the PCBM with a time constant of 50 ps. This finding indicates that almost all the introduced SiPc6 molecules are in close contact with both P3HT and PCBM, i.e., are segregated at the interface between P3HT and PCBM. This spontaneous interfacial segregation of the SiPc6 molecules indicates that there should be some self-organized segregation driving forces. On the basis of some modeling studies, we found that P3HT crystallization excludes SiPc6 molecules from the interface and that the surface energy of the SiPc6 molecules is between those of P3HT and PCBM, thereby inducing interface segregation. We further systematically studied the relationship between the surface energy and the location of near-IR dye molecules in RRa-P3HT/PS blend films. We found that BuSiPc6 with a lower surface energy incorporating hexyl and tertiary butyl groups is located in the P3HT domain with a smaller surface energy, SiPcBz with a higher surface energy incorporating benzyl groups is located in the PS domains with a higher surface energy, and SiPc6 with an intermediate surface energy is spontaneously segregated at the RRa-P3HT/PS interface. These results indicate that the hexyl group is compatible with lower surface energy P3HT and that the benzyl group is compatible with higher surface energy PCBM. We therefore synthesized a heterostructured near-IR dye molecule, SiPcBz6, with both hexyl and benzyl groups, which are compatible with P3HT and PCBM, respectively. As a result, the PCE also improved by approximately 30% in RR-P3HT/PCBM/SiPcBz6 ternary blend polymer solar cells. This occurred because the J_{SC} linearly increased up to a higher concentration of 15 wt%, which is three times greater than that of the device with conventional homostructured near-IR dye molecules. This finding suggests that SiPcBz6 can be spontaneously segregated even at concentrations up to 15 wt%. Thus, while only a small amount of near-IR dye molecules can be introduced into ternary blend polymer solar cells, as discussed in ref. [64], careful molecular design can overcome this limitation. Additionally, a recent study has shown that the light-harvesting efficiency can be effectively improved even with only a small amount of near-IR molecules by using optical interference effects in a thick active layer with high-charge-mobility conjugated polymers [86]. Furthermore, ternary blend polymer solar cells can induce better ordering of conjugated polymer chains and improve charge transport, resulting in improved FF

in addition to J_{SC}. Considering that recently, highly efficient polymer solar cells with high PCEs of >20% have adopted ternary blend polymer solar cells, ternary blend devices are expected to contribute to even higher PCEs as a standard device structure for highly efficient polymer solar cells.

Acknowledgements The author is grateful to all the collaborators for contributing to this research project. In particular, he would like to express his deepest gratitude to Dr. Satoshi Honda, Dr. Huajun Xu, and Dr. Hyung Do Kim for their core contributions. This work was partly supported by the JST PRESTO program (Photoenergy Conversion Systems and Materials for the Next Generation Solar Cells) and the JST ALCA grogram (JPMJAL1404) and was also supported by JSPS KAKENHI (JP19K22217, JP21H04692).

Compliance with ethical standards

Conflict of interest The author declares no competing interests.

References

1. Tang CW. Two-layer organic photovoltaic cell. Appl Phys Lett. 1986;48:183–5.
2. Tang CW, VanSlyke SA. Organic electroluminescent diodes. Appl Phys Lett. 1987;51:913–5.
3. Hiramoto M, Fujiwara H, Yokoyama M. Three-layered organic solar cell with a photoactive interlayer of codeposited pigments. Appl Phys Lett. 1991;58:1062–4.
4. Yu G, Gao J, Hummelen JC, Wudl F, Heeger AJ. Polymer photovoltaic cells: enhanced efficiencies via a network of internal donor-acceptor heterojunction. Science. 1995;270:1789–91.
5. Halls JJM, Walsh CA, Greenham NC, Marseglla EA, Friend RH, Moratti SC, et al. Efficient photodiodes from interpenetrating polymer networks. Nature. 1995;376:498–500.
6. Wang J, Zheng Z, Bi P, Chen Z, Wang Y, Liu X, et al. Tandem organic solar cells with 20.6% efficiency enabled by reduced voltage losses. Natl Sci Rev. 2023;10:nwad085.
7. Wang L, Chen C, Gan Z, Cheng J, Sun Y, Zhou J, et al. Diluted ternary heterojunctions to suppress charge recombination for organic solar cells with 21% efficiency. Adv Mater. 2025;37:2419923.
8. Shaheen SE, Brabec CJ, Sariciftci NS, Padinger F, Fromherz T, Hummelen JC. 2.5% Efficient organic plastic solar cells. Appl Phys Lett. 2001;78:841–3.
9. Wienk MM, Kroon JM, Verhees WJH, Knol J, Hummelen JC, van Hal PA, et al. Efficient methano[70]fullerene/MDMO-PPV bulk heterojunction photovoltaic cells. Angew Chem Int Ed. 2003;42:3371–5.
10. Padinger F, Rittberger RS, Sariciftci NS. Effects of postproduction treatment on plastic solar cells. Adv Funct Mater. 2003;13:85–88.
11. Ma W, Yang C, Gong X, Lee K, Heeger AJ. Thermally stable, efficient polymer solar cells with nanoscale control of the interpenetrating network morphology. Adv Funct Mater. 2005;15:1617–22.
12. Li G, Shrotriya V, Huang J, Yao Y, Moriarty T, Emery K, et al. High-efficiency solution processable polymer photovoltaic cells by self-organization of polymer blends. Nat Mater. 2005;4:864–8.
13. Kim Y, Cook S, Tuladhar SM, Choulis SA, Nelson J, Durrant JR, et al. A strong regioregularity effect in self-organizing conjugated polymer films and high-efficiency polythiophene:fullerene solar cells. Nat Mater. 2006;5:197–203.
14. Kim JY, Kim SH, Lee HH, Lee K, Ma W, Gong X, et al. New architecture for high-efficiency polymer photovoltaic cells using solution-based titanium oxide as an optical spacer. Adv Mater. 2006;18:572–6.
15. Irwin MD, Buchholz B, Hains AW, Chang RPH, Marks TJ. *p*-Type semiconducting nickel oxide as an efficiency-enhancing anode interfacial layer in polymer bulk-heterojunction solar cells. PNAS. 2008;105:2783–7.
16. Peet J, Kim JY, Coates NE, Ma WL, Moses D, Heeger AJ, et al. Efficiency enhancement in low-bandgap polymer solar cells by processing with alkane dithiols. Nat Mater. 2007;6:497–500.
17. Liang Y, Wu Y, Feng D, Tsai ST, Son HJ, Li G, et al. Development of new semiconducting polymers for high performance solar cells. J Am Chem Soc. 2009;131:56–57.
18. Liang Y, Feng D, Wu Y, Tsai ST, Li G, Ray C, et al. Highly efficient solar cell polymers developed via fine-tuning of structural and electronic properties. J Am Chem Soc. 2009;131:7792–9.
19. Hou J, Chen HY, Zhang S, Chen RI, Yang Y, Wu Y, et al. Synthesis of a low band gap polymer and its application in highly efficient polymer solar cells. J Am Chem Soc. 2009;131:15586–7.
20. Chen HY, Hou J, Zhang S, Liang Y, Yang G, Yang Y, et al. Polymer solar cells with enhanced open-circuit voltage and efficiency. Nat Photon. 2009;3:649–53.
21. He Z, Zhong C, Su S, Xu M, Wu H, Cao Y. Enhanced power-conversion efficiency in polymer solar cells using an inverted device structure. Nat Photon. 2012;6:591–5.
22. Liao SH, Jhuo HJ, Yeh PN, Cheng YS, Li YL, Lee YH, et al. Single junction inverted polymer solar cell reaching power conversion efficiency 10.31% by employing dual-doped zinc oxide nano-film as cathode interlayer. Sci Rep. 2014;4:6813.
23. Liu Y, Zhao J, Li Z, Mu C, Ma W, Hu H, et al. Aggregation and morphology control enables multiple cases of high-efficiency polymer solar cells. Nat Commun. 2014;5:5293.
24. Chen JD, Cui C, Li YQ, Zhou L, Ou QD, Li C, et al. Single-junction polymer solar cells exceeding 10% power conversion efficiency. Adv Mater. 2014;27:1035–41.
25. He Z, Xiao B, Liu F, Wu H, Yang Y, Xiao S, et al. Single-junction polymer solar cells with high efficiency and photovoltage. Nat Photon. 2015;9:174–9.
26. Vohra V, Kawashima K, Kakara T, Koganezawa T, Osaka I, Takimiya K, et al. Efficient inverted polymer solar cells employing favourable molecular orientation. Nat Photon. 2015;9:403–9.
27. Zhai J, Li Y, Yang G, Jiang K, Lin H, Ade H, et al. Efficient organic solar cells processed from hydrocarbon solvents. Nat Energy. 2016;1:15027.
28. Li S, Ye L, Zhao W, Zhang S, Mukherjee S, Ade H, et al. Energy-level modulation of small-molecule electron acceptors to achieve over 12% efficiency in polymer solar cells. Adv Mater. 2016;28:9423–9.

29. Zhao W, Li S, Yao H, Zhang S, Zhang Y, Yang B, et al. Molecular optimization enables over 13% efficiency in organic solar cells. J Am Chem Soc. 2017;139:7148–51.
30. Li W, Ye L, Li S, Yao H, Ade H, Hou J. A high-efficiency organic solar cell enabled by the strong intramolecular electron push–pull effect of the nonfullerene acceptor. Adv Mater. 2018;30:1707170.
31. Zhang S, Qin Y, Zhu J, Hou J. Over 14% efficiency in polymer solar cells enabled by a chlorinated polymer donor. Adv Mater. 2018;30:1800868.
32. Li S, Ye L, Zhao W, Yan H, Yang B, Liu D, et al. A wide band gap polymer with a deep highest occupied molecular orbital level enables 14.2% efficiency in polymer solar cells. J Am Chem Soc. 2018;140:7159–67.
33. Yuan J, Zhang Y, Zhou L, Zhang G, Yip HL, Lau TK, et al. Single-junction organic solar cell with over 15% efficiency using fused-ring acceptor with electron-deficient core. Joule. 2019;3:1140–51.
34. Liu Q, Jiang Y, Jin K, Qin J, Xu J, Li W, et al. 18% Efficiency organic solar cells. Sci Bull. 2020;65:272–5.
35. Meng H, Liao C, Deng M, Xu X, Yu L, Peng Q. 18.77% Efficiency organic solar cells promoted by aqueous solution processed cobalt(II) acetate hole transporting layer. Angew Chem Int Ed. 2021;60:22554–61.
36. Cui Y, Xu Y, Yao H, Bi P, Hong L, Zhang J, et al. Single-junction organic photovoltaic cell with 19% efficiency. Adv Mater. 2021;33:2102420.
37. He C, Pan Y, Ouyang Y, Shen Q, Gao Y, Yan K, et al. Manipulating the D:A interfacial energetics and intermolecular packing for 19.2% efficiency organic photovoltaics. Energy Environ Sci. 2022;15:2537–44.
38. Zhu L, Zhang M, Xu J, Li C, Yan J, Zhou G, et al. Single-junction organic solar cells with over 19% efficiency enabled by a refined double-fibril network morphology. Nat Mater. 2022;21:656–63.
39. Wei Y, Chen Z, Lu G, Yu N, Li C, Gao J, et al. Binary organic solar cells breaking 19% via manipulating the vertical component distribution. Adv Mater. 2022;34:2204718.
40. Jiang Y, Sun S, Xu R, Liu F, Miao X, Ran G, et al. Non-fullerene acceptor with asymmetric structure and phenyl-substituted alkyl side chain for 20.2% efficiency organic solar cells. Nat Energy. 2024;4:975–86.
41. Chen Z, Ge J, Song W, Tong X, Liu H, Yu X, et al. 20.2% Efficiency organic photovoltaics employing a π-extension quinoxaline-based acceptor with ordered arrangement. Adv Mater. 2024;36:2406690.
42. Yi J, Zhang G, Yu H, Yan H. Advantages, challenges and molecular design of different material types used in organic solar cells. Nat Rev Mater. 2024;9:46–62.
43. Yang N, Zhang S, Cui Y, Wang J, Cheng S, Hou J. Molecular design for low-cost organic photovoltaic materials. Nat Rev Mater. 2025;10:404–24.
44. Honda S, Nogami T, Ohkita H, Benten H, Ito S. Improvement of the light-harvesting efficiency in polymer/fullerene bulk heterojunction solar cells by interfacial dye modification. ACS Appl Mater Interfaces. 2009;1:804–10.
45. Xu H, Wada T, Ohkita H, Benten H, Ito S. Dye sensitization of polymer/fullerene solar cells incorporating bulky phthalocyanines. Electrochim Acta. 2013;100:214–9.
46. Honda S, Ohkita H, Benten H, Ito S. Multi-colored dye sensitization of polymer/fullerene bulk heterojunction solar cells. Chem Commun. 2010;46:6596–8.
47. Honda S, Yokoya S, Ohkita H, Benten H, Ito S. Light-harvesting mechanism in polymer/fullerene/dye ternary blends studied by transient absorption spectroscopy. J Phys Chem C. 2011;115:11306–17.
48. Honda S, Ohkita H, Benten H, Ito S. Selective dye loading at the heterojunction in polymer/fullerene solar cells. Adv Energy Mater. 2011;1:588–98.
49. Xu H, Wada T, Ohkita H, Benten H, Ito S. Molecular design of near-IR dyes with different surface energy for selective loading to the heterojunction in blend films. Sci Rep. 2015;5:9321.
50. Xu H, Ohkita H, Tamai Y, Benten H, Ito S. Interface engineering for ternary blend polymer solar cells with a heterostructured near-IR dye. Adv Mater. 2015;27:5868–74.
51. Wang Y, Zheng B, Tamai Y, Ohkita H, Benten H, Ito S. Dye sensitization in the visible region for low-bandgap polymer solar cells. J Electrochem Soc. 2014;161:D3093–D3096.
52. Wang Y, Ohkita H, Benten H, Ito S. Highly efficient exciton harvesting and charge transport in ternary blend solar cells based on wide- and low-bandgap polymers. Phys Chem Chem Phys. 2015;17:27217–24.
53. Kim HD, Shimizu R, Ohkita H. Ternary blend polymer solar cells based on wide-bandgap polymer PDCBT and low-bandgap polymer PTB7-Th. Chem Lett. 2018;47:1059–62.
54. Midori K, Fukuhara T, Tamai Y, Kim HD, Ohkita H. Enhanced hole transport in ternary blend polymer solar cells. ChemPhysChem. 2019;20:2683–8.
55. Kim HD, Iriguchi R, Fukuhara T, Benten H, Ohkita H. Enhanced charge transport in a conjugated polymer blended with an insulating polymer. Chem Asian J. 2020;15:796–801.
56. Ito S, Ohkita H, Benten H, Honda S. Near-IR dye sensitization in bulk heterojunction polymer solar cells. ECS Trans. 2012;41:27–34.
57. Wang Y, Ohkita H, Benten H, Ito S. Near-IR sensitization of polymer solar cells incorporating low-bandgap small molecule. Trans Mater Soc Jpn. 2014;39:439–42.
58. Xu H, Ohkita H, Hirata T, Benten H, Ito S. Near-IR dye sensitization of polymer solar cells. Polymer. 2014;55:2856–60.
59. Xu H, Ohkita H, Benten H, Ito S. Open-circuit voltage of ternary blend polymer solar cells. Jpn J Appl Phys. 2014;53:01AB10.
60. Wang Y, Chen J, Kim HD, Wang B, Iriguchi R, Ohkita H. Ternary blend solar cells based on a conjugated polymer with diketopyrrolopyrrole and carbazole units. Front Energy Res. 2018;6:113.
61. Peet J, Tamayo AB, Dang XD, Seo JH, Nguyen TQ. Small molecule sensitizers for near-infrared absorption in polymer bulk heterojunction solar cells. Appl Phys Lett. 2008;93:163306.
62. Ameri T, Khoram P, Min J, Brabec CJ. Organic ternary solar cells: a review. Adv Mater. 2013;25:4245–66.
63. Lu L, Kelly MA, You W, Yu L. Status and prospects for ternary organic photovoltaics. Nat Photon. 2015;9:491–500.
64. Savoie BM, Dunaisky S, Marks TJ, Ratner MA. The scope and limitations of ternary blend organic photovoltaics. Adv Energy Mater. 2015;5:1400891.
65. An Q, Zhang F, Zhang J, Tang W, Deng Z, Hu B. Versatile ternary organic solar cells: a critical review. Energy Environ Sci. 2016;9:281–322.
66. Huang W, Cheng P, Yang YM, Li G, Yang Y. High-performance organic bulk-heterojunction solar cells based on multiple-donor or multiple-acceptor components. Adv Mater. 2018;30:1705706.
67. Li H, Lu K, Wei Z. Polymer/small molecule/fullerene based ternary solar cells. Adv Energy Mater. 2017;7:1602540.
68. Liu X, Yan Y, Yao Y, Liang Z. Ternary blend strategy for achieving high-efficiency organic solar cells with nonfullerene acceptors involved. Adv Funct Mater. 2018;28:1802004.
69. Xu W, Gao F. The progress and prospects of non-fullerene acceptors in ternary blend organic solar cells. Mater Horiz. 2018;5:206–21.
70. Fu H, Wang Z, Sun Y. Advances in non-fullerene acceptor based ternary organic solar cells. Sol RRL. 2018;2:1700158.
71. Gasparini N, Salleo A, McCulloch I, Baran D. The role of the third component in ternary organic solar cells. Nat Rev Mater. 2019;4:229–42.

72. Mohapatra AA, Tiwari V, Patil S. Energy transfer in ternary blend organic solar cells: recent insights and future directions. Energy Environ Sci. 2021;14:302–19.
73. Xu X, Li Y, Peng Q. Ternary blend organic solar cells: understanding the morphology from recent progress. Adv Mater. 2022;34:2107476.
74. Ltaief A, Chaâbane RB, Bouazizi A, Davenas J. Photovoltaic properties of bulk heterojunction solar cells with improved coverage. Mater Sci Eng C. 2006;26:344–7.
75. Dastoor PC, McNeill CR, Frohne H, Foster CJ, Dean B, Fell CJ, et al. Understanding and improving solid-state polymer/C_{60}-fullerene bulk-heterojunction solar cells using ternary porphyrin blends. J Phys Chem C. 2007;111:15415–26.
76. Huang JS, Goh T, Li X, Sfeir MY, Bielinski EA, Tomasulo S, et al. Polymer bulk heterojunction solar cells employing Förster resonance energy transfer. Nat Photon. 2013;7:479–85.
77. Gupta V, Bharti V, Kumar M, Chand S, Heeger AJ. Polymer–polymer Förster resonance energy transfer significantly boosts the power conversion efficiency of bulk-heterojunction solar cells. Adv Mater. 2015;27:4398–404.
78. Sumita M, Sakata K, Asai S, Miyasaka K, Nakagawa H. Dispersion of fillers and the electrical conductivity of polymer blends filled with carbon black. Polym Bull. 1991;25:265–71.
79. Li D, Neumann AW. A reformulation of the equation of state for interfacial tensions. J Colloid Interface Sci. 1990;137:304–7.
80. Gasparini N, Jiao X, Heumueller T, Baran D, Matt GJ, Fladischer S, et al. Designing ternary blend bulk heterojunction solar cells with reduced carrier recombination and a fill factor of 77%. Nat Energy. 2016;1:16118.
81. Lee J, Tamilavan V, Rho KH, Keum S, Park KH, Han D, et al. Overcoming fill factor reduction in ternary polymer solar cells by matching the highest occupied molecular orbital energy levels of donor polymers. Adv Energy Mater. 2017;8:1702251.
82. Nian L, Kan Y, Wang H, Gao K, Xu B, Rong Q, et al. Ternary non-fullerene polymer solar cells with 13.51% efficiency and a record-high fill factor of 78.13%. Energy Environ Sci. 2018;11:3392–9.
83. Li Z, Ying L, Xie R, Zhu P, Li N, Zhong W, et al. Designing ternary blend all-polymer solar cells with an efficiency of over 10% and a fill factor of 78. Nano Energy. 2018;51:434–41.
84. An Q, Wang J, Zhang F. Ternary polymer solar cells with alloyed donor achieving 14.13% efficiency and 78.4% fill factor. Nano Energy. 2019;60:768–74.
85. Zeng Y, Li D, Xiao Z, Wu H, Chen Z, Hao T, et al. Exploring the charge dynamics and energy loss in ternary organic solar cells with a fill factor exceeding 80%. Adv Energy Mater. 2021;11:2101338.
86. Saito M, Tamai Y, Ichikawa H, Yoshida H, Yokoyama D, Ohkita H, et al. Significantly sensitized ternary blend polymer solar cells with a very small content of the narrow-band gap third component that utilizes optical interference. Macromolecules. 2020;53:10623–35.

Hideo Ohkita is a professor in the Department of Polymer Chemistry at Kyoto University. He received his PhD degree from Kyoto University in 1997. He was appointed as an assistant professor in 1997, promoted to associate professor in 2006, and became a professor in the Department of Polymer Chemistry at Kyoto University in 2016. From 2005 to 2006, he worked as an academic visitor under Professor Durrant at Imperial College London. Additionally, from 2009 to 2015, he concurrently served as a researcher in the Precursory Research for Embryonic Science and Technology (PRESTO) program of Japan Science and Technology Agency (JST), focusing on "Photoenergy Conversion Systems and Materials for the Next Generation Solar Cells". He received the Japanese Photochemistry Association Award in 2018 and the Award of the Society of Polymer Science, Japan in 2023. His primary research fields are the study of photophysics and photochemistry in polymer systems. His current research focuses on spectroscopic and device physics approaches related to polymer solar cells.